

CoSWAT Model v1: A High-Resolution Global SWAT+ Hydrological Model for Impact Studies.

Celray James Chawanda^{1,2}, Ann van Griensven^{1,3}, Albert Nkwasa^{1,4}, Jose Pablo Teran Orsini¹, Jaehak
5 Jeong², Soon-Kun Choi⁵, Raghavan Srinivasan², Jeffrey G. Arnold⁶,

¹ Department of Water and Climate, Vrije Universiteit Brussel, Elsene, 1050, Belgium

² Blackland Research & Extension Center, Texas A&M AgriLife Research, Temple, 76502 TX, USA

³ Institute for Water Education (IHE) Delft, 2611 AX Delft, The Netherlands

⁴ International Institute for Applied Systems Analysis (IIASA), A-2361 Laxenburg, Austria

10 ⁵ National Institute of Agricultural Sciences (NAS), Rural Development Administration, Republic of Korea

⁶ Grassland Soil and Water Research Laboratory, USDA Agricultural Research Service (ARS), Temple, 76502 TX, USA

Correspondence to: Celray James Chawanda (celray.chawanda@tamu.edu)

Abstract

Global hydrological models are essential tools for understanding water resources and assessing Climate Change (CC) impacts at planetary scales, supporting water management, flood risk assessment, and sustainable development initiatives worldwide. The Soil and Water Assessment Tool (SWAT+) has demonstrated robust performance across various environments and scales, from local to continental applications. However, despite its widespread use, a global implementation of SWAT+ is currently lacking due to computational demands and data management challenges, while existing global models often lack the detailed process representation and high spatial resolution needed for comprehensive hydrological analysis. A global SWAT+ model would offer unique advantages through its integrated simulation of water quantity, quality, and land management processes, while supporting multiple UN Sustainable Development Goals and enhancing research opportunities in global hydrology. This study aimed to develop a High-resolution Global SWAT+ Model and establish a reproducible framework for large-scale SWAT+ applications. We developed the Community SWAT (CoSWAT) modeling framework, an open-source solution that automates data retrieval, preprocessing, and model configuration using Python, while maximizing parallel processing for computational efficiency. The global model was then set up using the framework at 2km resolution using ASTER DEM, ESA land use data, FAO soil data, and ISIMIP climate data, with performance evaluated against GRDC flow data and GLEAM evapotranspiration dataset. Results without calibration showed reasonable spatial patterns in evapotranspiration simulation with 78.54% of sampled points showing differences within $\pm 100\text{mm}$ compared to GLEAM data, though river discharge performance was limited due to lack of reservoir implementation with 23.02% of stations showing positive Kling-Gupta Efficiency values. The development of this first global SWAT+ model demonstrates the feasibility of high-resolution global hydrological modeling using SWAT+, while

the CoSWAT framework provides a robust foundation for reproducible large-scale modeling. These advances enable more detailed analysis of global water resources and CC impacts, though future work should focus on incorporating water management practices, improving process representation with calibration, and enhancing computational efficiency.

35 **1. Introduction**

Global water models aim to simulate phenomena at planetary scale. There are several global models that simulate the water cycle such as Global Hydrological Models (GHMs), Land Surface Models (LSMs), and Global Dynamic Vegetation Models (GDVMs), each of them with different approaches and purposes. Most models are based on a gridded structure and vary in how they represent water storage components and terrestrial processes. Nearly all models incorporate canopy, snow, and soil 40 water storage to some degree. Surface runoff is estimated by most models, while only a smaller group—specifically GHMs and a number of LSMs—include river routing to enable streamflow simulations. Additionally, only a small fraction of models account for reservoirs, with an even smaller subset incorporating lake and wetland storage (Telteu et al., 2021).

In order to assess water resources on a global scale, multi-model comparisons exist due to the differences in structures and 45 approaches of global water models. There are some Model Intercomparison Projects (MIPs) that focus on global water models such as the WaterMIP (Haddeland et al., 2011), and the Inter-Sectoral Impact Model Inter-Comparison Project (ISIMIP) that, on the ISIMIP 2 and 3 simulation rounds (Gosling et al., 2023a, b, 2024a, b), involves several models including GHMs, LSMs and DGVMs, as shown in Table 1.

50 **Table 1: Global Water Models utilized in the global water sector of ISIMIP**

Nr	Name	Category	Reference
1	CWatM	GHM	(Burek et al., 2020)
2	DBH	GHM	(Tang et al., 2007)
3	H08	GHM	(Hanasaki et al., 2018a)
4	HydroPy	GHM	(Stacke and Hagemann, 2021)
5	MPI-HM	GHM	(Stacke and Hagemann, 2012)
6	PCR-GLOBWB	GHM	(Sutanudjaja et al., 2018)
7	VIC	GHM	(Liang et al., 1994)
8	WaterGAP2	GHM	(Müller Schmied et al., 2021)
9	WAYS	GHM	(Mao and Liu, 2019)
10	WEB-DHM-SG	GHM/LSM	(Qi et al., 2022b)
11	CLASSIC	LSM	(Melton et al., 2020)
12	CLM 4.5	LSM	(Oleson et al., 2013)
13	CLM 5.0	LSM	(Lawrence et al., 2019)
14	ELM-ECA	LSM	(Zhu et al., 2019)
15	JULES	LSM	(Best et al., 2011)
16	MATSIRO	LSM	(Takata et al., 2003)
17	ORCHIDEE	LSM	(Guimberteau et al., 2014, 2017)

18	SWBM	LSM	(Rene Orth and Seneviratne, 2015)
19	SSiB4/TRIFFID	LSM/DGVM	(Huang et al., 2020)
20	LPJmL	DGVM	(Sitch et al., 2003)

Among these models, generally, GHMs focus on representing the land water balance, with particular emphasis on streamflow for model evaluation, while LSMs focus on the vertical exchange of energy and water between land and atmosphere, and DGVMs simulate global vegetation dynamics, where hydrological processes play an important role (Telteu et al., 2021).

Within the ISIMIP ensemble (Table 1), various models exemplify different categories. For instance, GHMs like (Burek et al., 2020) focus on water quantity assessment across sectors (Becher et al., 2024; Palazzo et al., 2024), H08 (Hanasaki et al., 2018a) maps water abstractions and availability, PCR-GLOBWB (Sutanudjaja et al., 2018) simulates the terrestrial water cycle including human influences (Becher et al., 2024; Burek et al., 2020; Palazzo et al., 2024), The Variable Infiltration Capacity (VIC) assesses human impacts on water resources (Liang et al., 1994), and WaterGAP (Müller Schmied et al., 2021) simulates runoff, recharge, and streamflow considering various storages. LSMs such as CLM, CLASSIC, JULES, and MATSIRO (Best et al., 2011; Lawrence et al., 2019; Melton et al., 2020; Takata et al., 2003) simulate broader land surface processes including energy, water, carbon fluxes, and vegetation dynamics, often incorporating hydrological components. DGVMs like LPJmL (Sitch et al., 2003) simulate vegetation dynamics and surface water balance, including human influences like irrigation. Despite differing primary objectives, these models are often used collectively in ensemble studies to assess Climate Change (CC) impacts on various hydrological aspects like groundwater recharge (Reinecke et al., 2021), river flow (Gudmundsson et al., 2021) and soil moisture (Porkka et al., 2024), river ecological functioning (Thompson et al., 2021), droughts (Kew et al., 2021; Pokhrel et al., 2021), and floods (Dottori et al., 2018; Tabari et al., 2021; Zhou et al., 2023), both globally and regionally.

Despite the differences in general purposes and focus for model development between LSMs, GHMs and DGVMs, as part as the model ensemble for the global water sector from ISIMIP (Table 1), they have been used together for several studies. On a global scale, model ensembles were used to study the future changes in groundwater recharge (Reinecke et al., 2021). They were applied to assess the historical and future impacts of CC on river flow trend and soil moisture (Gudmundsson et al., 2021; Porkka et al., 2024; Thompson et al., 2021). Moreover, others have studied historical and future changes in drought and flood risks, trends and impacts (Dottori et al., 2018; Kew et al., 2021; Pokhrel et al., 2021; Tabari et al., 2021; Zhou et al., 2023). On a regional scale, ensembles of models were used to study compound extreme climate events (Muheki et al., 2024), and project future indices regarding water scarcity in the context of CC and societal changes (Yin et al., 2020).

The ability to simulate water resources and the impacts of CC and other human induced environmental changes is indispensable in planning for and management of water resources (Ramteke et al., 2020; Soltani et al., 2023; Zhuang et al.,

2018). This is true for both small scales and large scales (Chawanda et al., 2024; Fu et al., 2019). By predicting how CC and other human drivers affect the water cycle, the models help in developing strategies to cope with droughts, floods and other water-related challenges (Brunner et al., 2021). Hydrological models also enable more effective management of water resources to optimize the use of water for agriculture (Li et al., 2020; Srivastava et al., 2020), industry, and human consumption, especially in regions where water is scarce (Hanasaki et al., 2018b). These models at a global level can also support global sustainable initiatives by ensuring that development projects align with long-term water availability (Amjath-Babu et al., 2019). At the same time, they can also offer means for forecasting extreme events like floods and droughts in any region of the world, thereby enhancing preparedness and allowing timely warning for disaster response efforts.

90 SWAT+ (Soil and Water Assessment Tool) is a completely revised version of the original SWAT model (Arnold et al., 2018; Bieger et al., 2017). It performs hydrological simulations at the Hydrologic Response Units (HRU) scale. HRUs represent unique combinations of land use, soil, and slope characteristics within each landscape unit or subbasin. The SWAT+ model can simulate a wide range of processes including surface runoff and infiltration, evapotranspiration ([ET](#)) and other water balance components (Pandi et al., 2023). SWAT+ also simulates Soil Erosion and Sediment Transport, Nutrient Cycle and 95 Land Use and Management Practices (Arnold et al., 2018). SWAT has been applied all over the world in various environments including in Temperate (Qi et al., 2019), Tropical and Subtropical (Alemayehu et al., 2017; Ma et al., 2019), Arid and Semi-Arid (Samimi et al., 2020), Mediterranean Climates, Cold and Mountainous Regions, Wetlands and even Coastal Environments (Peker and Sorman, 2021; Pulighe et al., 2021; Upadhyay et al., 2022). SWAT+ has also been applied at small scales (Qi et al., 2022a), regional scale (Chawanda et al., 2020a; Nkwasa et al., 2022b) and even continental scale 100 (Abbaspour et al., 2015; Chawanda et al., 2024; Nkwasa et al., 2024).

105 Despite such applications, there are no global applications at present because as with other global modelling efforts, large-scale SWAT+ applications face several significant challenges. Data availability and quality remain a challenge (Crochemore et al., 2020). High-resolution, consistent, and up-to-date datasets for land use, soil properties, and climate variables are often lacking or incomplete (Chawanda et al., 2024; Döll et al., 2016), particularly in developing regions which can lead to increased uncertainty in model outputs (Sood & Smakhtin, 2015) and limit the model's applicability. Computational demands 110 pose another challenge (Ma et al., 2023; Zhang et al., 2016). The computational requirements of setting up fine resolution SWAT+ model, running, calibrating and validating it, coupled with the storage resources required for the input and output data, necessitates significant computational resources. These two in addition to data processing methods used in global applications, can make it challenging to replicate and reuse any model set-ups available in a study area (Chawanda et al., 2020b). This issue may be compounded by frequent updates to model structure and parameters (Smith et al., 2020), which can lead to inconsistencies between studies conducted at different times. This calls for archiving and versioning systems in workflows for better reproducibility (Knoben et al., 2022).

While challenges persist, a global SWAT+ model is in a unique position to provide comprehensive insights into large-scale
115 processes across diverse ecosystems worldwide. To begin with, a global SWAT+ model offers a holistic approach in simulation of water quantity and quality, integrating detailed hydrological processes, nutrient cycling, and sediment transport (Abbaspour et al., 2015; Liu et al., 2017). The model also would enable high-resolution projections of climate change impacts on global water systems, critical for contributing to international assessments like Intergovernmental Panel on Climate Change (IPCC) reports. In addition, the global SWAT+ model directly supports multiple United Nations Sustainable
120 Development Goals (SDGs), by providing data crucial for balancing development with environmental conservation through simulation of Land Use and Land Cover Change (LULCC) and nutrients in water bodies. Implementing a global SWAT+ model also creates a standardised dataset for cutting-edge international research in hydrology, thereby enhancing research and educational opportunities. The model has significant implications in designing and enhancing the effectiveness of long-term global water and land management practices by allowing detailed simulations of global agricultural practices, land use
125 changes, and their water resource impacts.

The primary aim of this study was to develop a High-resolution Global SWAT+ Model, addressing the growing need for comprehensive, large-scale hydrological simulations. To achieve this overarching goal, we first establish a robust framework for setting up a high-resolution global SWAT+ model based on the study by Chawanda et. al., (2020b), ensuring
130 reproducibility and scalability of the model. This framework integrates global data processing methods and computational strategies that overcome the challenges inherent in global-scale modelling. Subsequently, we evaluate the model's performance against observed data. This evaluation not only benchmarks the Global SWAT+ Model's capabilities, but also identifies areas for potential refinement, contributing to the advancement of global hydrological modelling techniques.

2.1 Global Datasets for SWAT+

While setting up the global SWAT+ model, global data sources were used as input and for model evaluation.

2.1.1 Digital Elevation Model

The Advanced Spaceborne Thermal Emission and Reflection Radiometer (ASTER) global DEM (Abrams, 2016) was preferred over the Shuttle Radar Topography Mission (SRTM) global DEM (Farr et al., 2007) primarily due to its more complete global spatial coverage (Fig. 1), which is essential for this study's domain. [SRTM data only cover over 80% of the Earth's land surface \(60°N–56°S\), while ASTER goes further North and South covering 99% of land surface \(Yue et al., 2017\).](#)

145

150

155

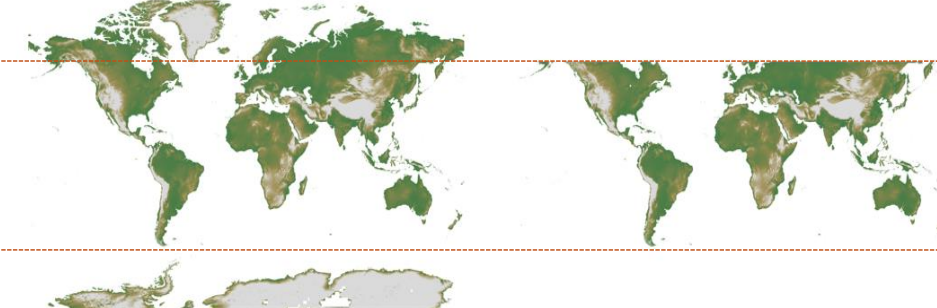
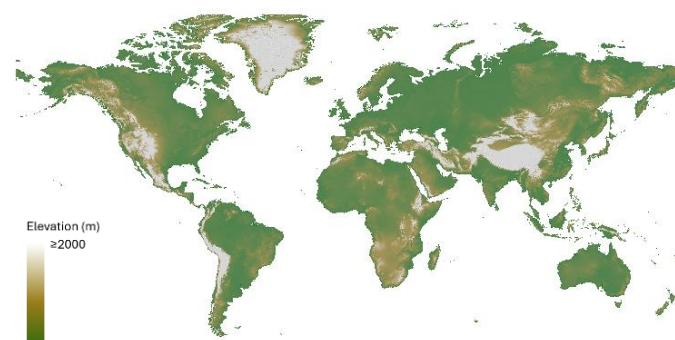
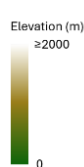
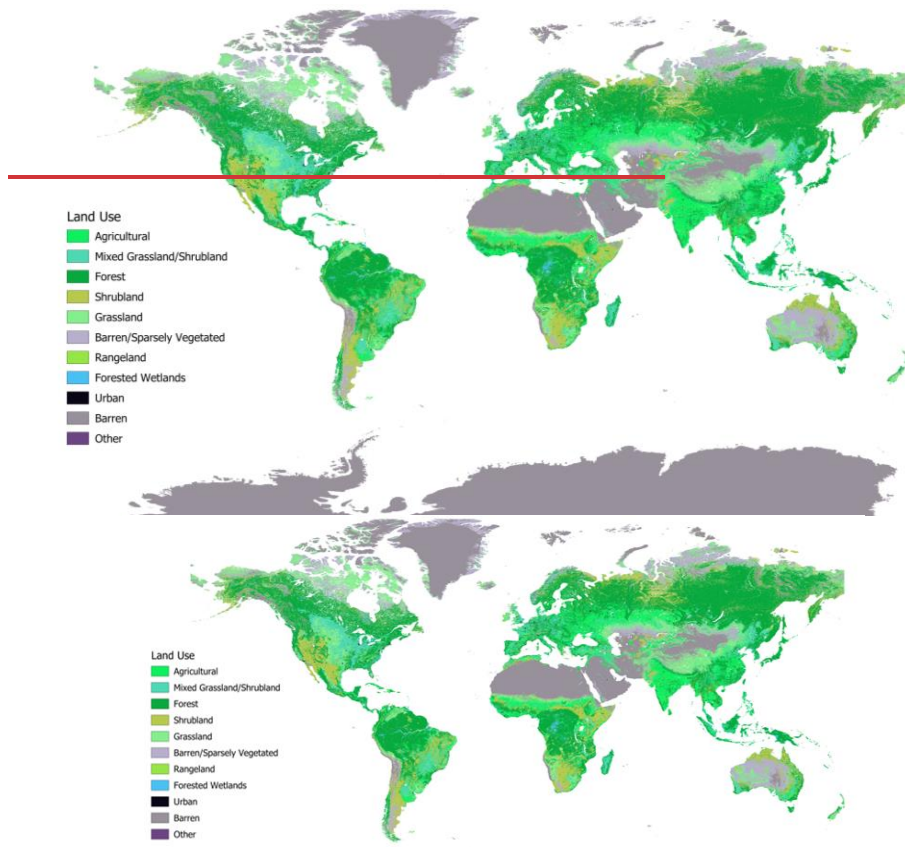


Figure 1: Spatial coverage of ASTER Global DEM ~~Excluding Antarctica (mapped at 2km resolution) vs SRTM. SRTM data only covers over 80% of the Earth's land surface (60°N–56°S), while ASTER goes further North and South (Yue et al., 2017).~~

160 While potential differences in DEM quality exist between the datasets, particularly in mountainous regions at finer native resolutions ~~of 30m~~, these differences are considered less critical at the 2km resolution used for deriving topographic parameters in this global model setup.

2.1.2 Land Use Map

165 ~~The land use data (Fig. 2) from the European Space Agency (ESA) is available at 300m resolution was downloaded from the ESA website (Defourny et al., 2017). The 2007 ESA land use map used for this study indicates that, excluding Antarctica, barren and sparsely vegetated areas dominate, accounting for over 32% of the global land surface. Grasslands and shrublands cover approximately 27%, while forests account for about 31%. Cropland represents around 7% of the global landmass. (ESA. Land Cover CCI Product User Guide Version 2. Tech. Rep. (2017). Available at: maps.elie.uel.ac.be/CCI/viewer/download/ESACCI_LC_Ph2_PUGv2_2.0.pdf)~~

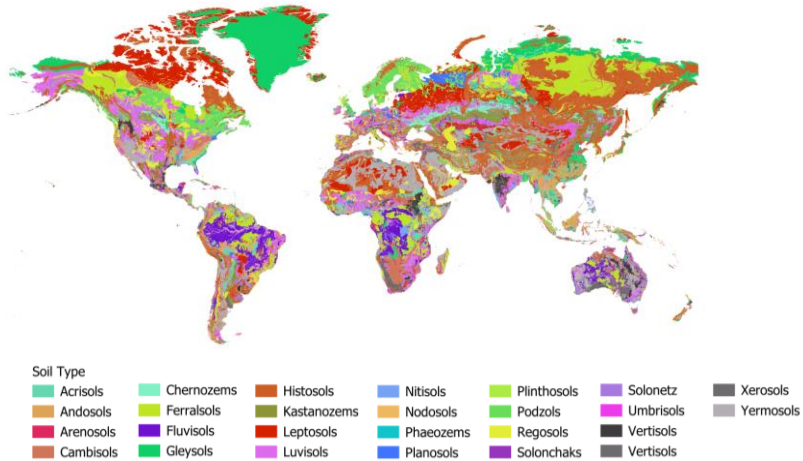


Formatted: Centered, Indent: Left: 0"

Figure 2: Major Land Use Categories ~~from~~ based on European Space Agency (ESA) 2007 Land Use Map

2.1.3 Soil Map

The FAO soil data (Fischer et al., 2008) was used in this study. The FAO soil data, particularly from the Harmonized World Soil Database (HWSD), provides global coverage of soil properties (Fig. 3) at a 1 km² resolution. The data is derived from multiple sources and is widely used in global and regional environmental studies, though it may lack precision for local-scale analysis due to the generalised nature of its source material.



Formatted: Indent: Left: 0"

180 **Figure 3: Global extent of FAO soil types** Major soil types (Fischer et al., 2008) from FAO Soil Map

2.1.4 Climate Data

Climate data was acquired from the GSWP3-EWEMBI reanalysis dataset (Lange and Büchner, 2020) through the Inter-Sectoral Impact Model Intercomparison (ISIMIP) project. The dataset contains historical climate data including daily minimum and maximum air temperature (tasmin and tasmax, respectively), precipitation (pr), relative humidity (rhs), solar radiation (rls), and near-surface wind speed (wind) at 0.5 decimal degrees [which corresponds to about 55.66 km along the equator](#).

185

2.1.5 River Flow Data

The monthly river flow for evaluation was acquired from The Global Runoff Data Centre (GRDC, <https://portal.grdc.bafg.de/applications/public.htm>). The gauging station location data was also used in the delineation to 190 create outlets in the model setups.

2.1.6 ET Data

GLEAM v4 dataset available at 0.1° resolution was used for evaluating ET (Miralles et al., 2025). The datasets require preprocessing to be used by the SWAT+ model. In our model set up, the preprocessing was done in the scripted workflow described in the next section.

195 **2.2 Scripted Workflow Modelling Framework for Global SWAT+ Setup**

To facilitate the setup of a global SWAT+ model, we developed a python based scripted workflow based on SWAT+ AW (Chawanda et al., 2020b). This new workflow, named the Community SWAT (CoSWAT) modelling framework (Fig. 4), is a free and open-source solution designed for large-scale modelling using SWAT+.

200 The framework simplifies the setup process for global SWAT+ models by automating data retrieval, pre-processing, and model configuration. The user is required to define regions of interest using box coordinates. Settings for model set up are saved in one file referred to as the 'configuration file'. Having model setup settings in one file ensures consistency across the global model. To ensure reproducibility and ease of use, the workflow includes stages for retrieving and preparing essential input datasets. These stages are automated and controlled by the configuration file settings:

205

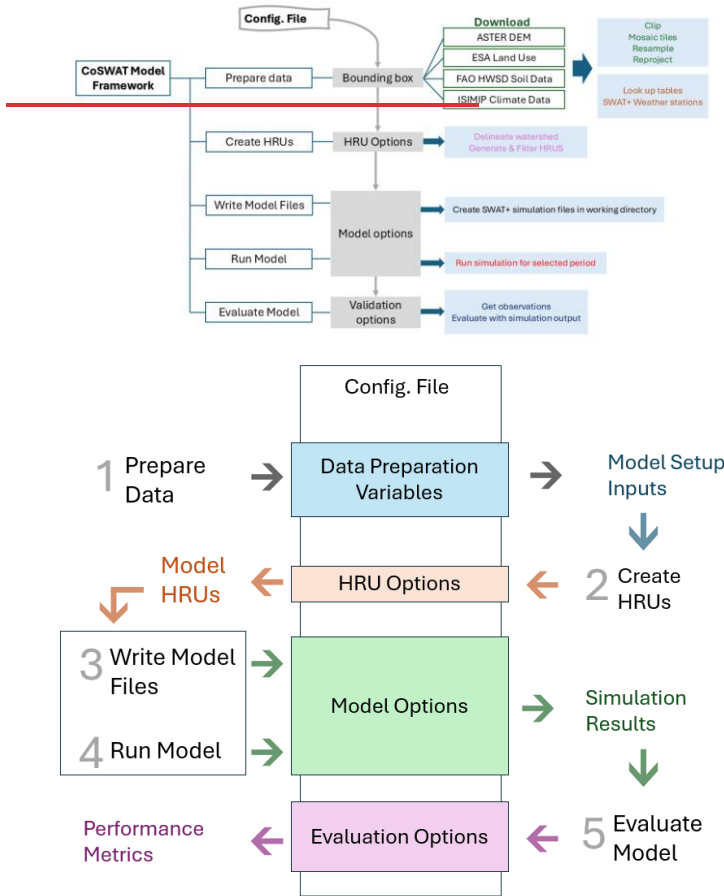
- Digital Elevation Model (DEM): The CoSWAT framework downloads ASTER DEM tiles, mosaics them into a continuous surface, and resamples and reprojects them as per the configuration file.
- Land Use Data: The framework automatically retrieves land use maps from the European Space Agency (ESA) and processes them. The data is resampled, and reprojected. The lookup file is manually prepared once. This is done by matching ESA land use classification to equivalent land use types in the SWAT+ land use database.
- Soil Data: Soil data from the FAO Harmonized World Soil Database (HWSD) is downloaded and transformed into the format required by SWAT+. The framework handles rasterization and reprojection to prepare the soil data into a format required by SWAT+. FAO soil lookup and soil properties database are readily available from the SWAT+ website (SWAT Global Data, 2025) through QSWAT+ Software and are used by the workflow.
- Climate Data: Climate inputs are downloaded from the ISIMIP dataset servers. The workflow processes historical and scenario-based climate data, including variables such as precipitation, temperature, wind speed, solar radiation and relative humidity and formats them for use in SWAT+ simulations. The downloaded files are in NetCDF format and are read and written using the xarray python library. Users can customise climate scenarios using the configuration file. It is also possible to specify the spatial resolution of the points at which climate time series are created.

210

215

Formatted: Space Before: 12 pt

Formatted: List Paragraph, Indent: Left: 0", Outline numbered + Level: 1 + Numbering Style: Bullet + Aligned at: 0.25" + Tab after: 0" + Indent at: 0.5"



220

Figure 4: Schematic of the Community SWAT (CoSWAT) modelling framework. The flowchart illustrates the scripted workflow designed to automate the setup, execution, and evaluation of large-scale SWAT+ models. The entire process is controlled by a single configuration file, ensuring consistency and reproducibility.

The framework simplifies the setup process for global SWAT+ models by automating data retrieval, pre-processing, and model configuration. The user is required to define regions of interest using box coordinates. Settings for model set up are saved in one file referred to as the 'configuration file'. Having model setup settings in one file ensures consistency across

225

the global model. To ensure reproducibility and ease of use, the workflow includes stages for retrieving and preparing essential input datasets. These stages are automated and controlled by the configuration file settings:

- Digital Elevation Model (DEM): The CoSWAT framework downloads ASTER DEM tiles, mosaics them into a continuous surface, and resamples and reprojects them as per the configuration file.
- Land Use Data: The framework automatically retrieves land use maps from the European Space Agency (ESA) and processes them. The data is resampled, and reprojected. The lookup file is manually prepared once. This is done by matching ESA land use classification to equivalent land use types in the SWAT+ land use database.
- Soil Data: Soil data from the FAO Harmonized World Soil Database (HWSD) is downloaded and transformed into the format required by SWAT+. The framework handles rasterization and reprojection to prepare the soil data into a format required by SWAT+. FAO soil lookup and soil properties database are readily available from the SWAT+ website (SWAT Global Data, 2025) and are used by the workflow.
- Climate Data: Climate inputs are downloaded from the ISIMIP dataset servers. The workflow processes historical and scenario-based climate data, including variables such as precipitation, temperature, wind speed, solar radiation and relative humidity and formats them for use in SWAT+ simulations. The downloaded files are in NetCDF format and are read and written using the xarray python library. Users can customise climate scenarios using the configuration file. It is also possible to specify the spatial resolution of the points at which climate time series are created.

The flexibility of the CoSWAT Framework allows users to easily switch data sources, depending on the project's requirements or data availability which makes the framework a robust and adaptable tool for large-scale modelling.

In addition to the model setup, the CoSWAT framework integrates evaluation and visualisation tools. A local web application was developed to serve as an interactive portal, allowing users to visualise model results and outputs in a user-friendly environment. This platform enhances the accessibility and interpretation of model results. The CoSWAT framework was optimised by iteratively implementing parallel processing wherever possible and feasible. This reduces the time required for data processing and model setup, making large-scale simulations feasible by leveraging High Performance Computing (HPC) environments which often allow highly parallelised workflows (Chawanda et al., 2020b).

The efficiency gains from parallel processing significantly reduce computation time, though actual runtimes depend heavily on the specific HPC hardware (CPU cores, clock speed, Input/Output (I/O) speed) and parallel configurations used. For context, using the 64-core, 3.00 GHz, 128 GB RAM Linux environment described below (Section 2.3), the CoSWAT framework setup phase (including data preprocessing, watershed delineation, HRU generation, and file writing – not including data download times) required approximately 12 minutes for a moderately sized region such as Save Basin in Africa, and about 1 hour 49 minutes for a large, complex region such as the Nile Basin. Executing a 10-year SWAT+ simulation for very large basins like the Amazon could take over 24 hours, with runtime strongly influenced by the requested output frequency (e.g., daily outputs requiring significantly more time due to I/O demands).

Formatted: Space Before: 12 pt

2.3 Global SWAT+ Model Implementation and Evaluation

260 The data resolution for DEM, land use and soil maps were set to 2km projected in ESRI:54003 (Miller World Cylindrical) projection. Climate data resolution was however set to 0.5 decimal degrees due to limitations on the number of files the operating system allowed (<= 10,000,000 files). The thresholds for stream and channel were set to 44 cells – an equivalent of 177.7 km².

265 The model was setup in a 64-core HPC Environment running at 3.00 GHz, with 128 GB Memory running Linux. To take advantage of parallel processing and easy data handling, the global model was setup by combining regions defined based on major river basins (Fig. 5). However, Greenland was not included in this version.



Figure 5: Partitioning of the world land mass into regions based on main river basins.

270 Using the CoSWAT framework, data was prepared, and a model set up for each of these regions using the configuration file options. Slope classes were not considered in creation of HRUs. The Model Files were written with the following options: [the Muskingum method was applied for channel routing, and Penman–Monteith was used for potential evapotranspiration estimation. A five-year warm-up period was set, and the model was run for the simulation period 1977–1990.](#)

Formatted: Space Before: 12 pt

275

Table 2: Model configuration options used when writing model files.

Formatted: Space Before: 12 pt

Routing Method	Muskingum
PET Estimation Method	Penman–Monteith
Warm up Period	5 years
Simulation Period	1977–1990

The version of SWAT+ used to run the global SWAT+ model setup is 60.5.7. The global model was not calibrated as that was beyond the scope of this study. We used the Kling-Gupta Efficiency (KGE) metric (Gupta et al., 2009) to evaluate the flow time series at the monthly timestep. The plotting of results and metric calculation was implemented within the CoSWAT
280 framework.

The Kling-Gupta Efficiency (KGE) metric provides a more nuanced assessment of model performance than conventional measures like R^2 or Bias alone. It is formulated to simultaneously account for three key components: the linear correlation between simulated and observed time series (r), the variability ratio – α , which compares the standard deviation of simulated values against observations, and the bias ratio – β , which evaluates the mean offset between simulated and observed values
285 (Gupta et al., 2009). KGE gives a balanced indication of how well the model reproduces both the overall magnitude and the temporal dynamics of observed flows. By considering these complementary aspects.

In addition to reporting the KGE values, we also present the underlying distributions of r , α , and β across all gauging stations. This helps to reveal a global picture of how the model simulations compare against observed data.



290 **Figure 6: Sampled points for measuring distribution of ET differences between GLEAM and SWAT+ output.**

We also evaluated the simulated mean annual ET against the GLEAM v4 dataset. This evaluation involved two approaches: (1) a comparison of the spatial patterns on global maps to assess the model's ability to capture large-scale ET variations, and (2) an analysis of the distribution of differences at specific locations. For the latter, ET differences (GLEAM - SWAT+) were calculated at numerous quasi-randomly selected sample points globally (Fig. 6) and their frequency distribution was plotted
295 to assess overall model bias and the concentration of differences around zero.

3. Results

In total, there were 2.63 million HRUs. [Figure 5](#)–[Figure 7](#) illustrates the level of discretisation that was achieved in creating HRUs.

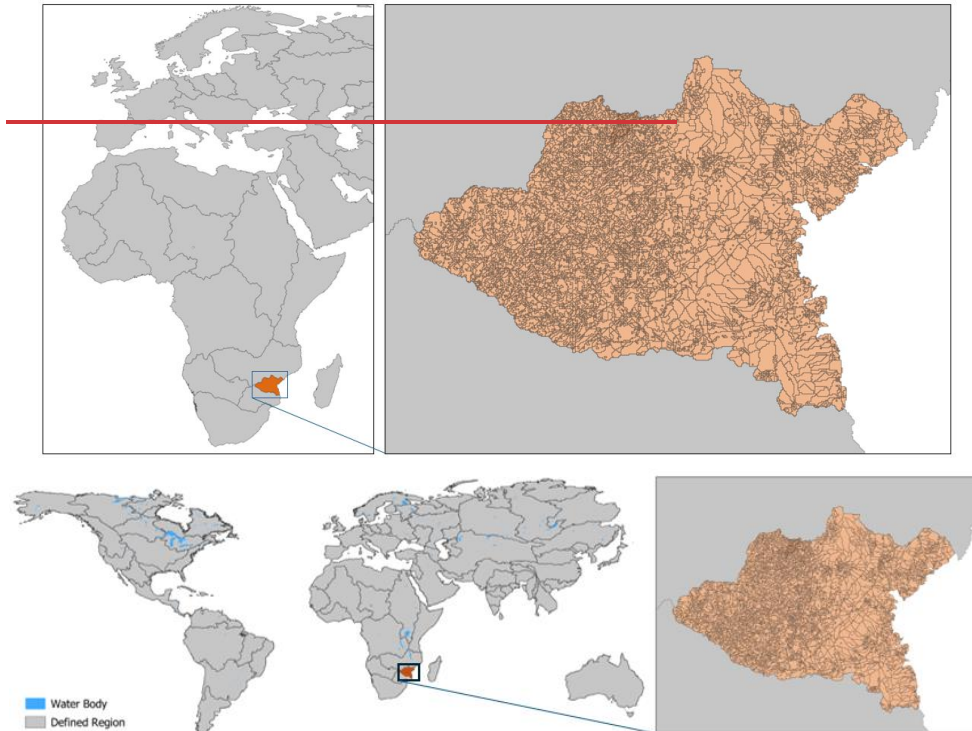


Figure 7: Illustration of density of HRUs in the Save Region of the African Continent

Figure 5: Partitioning of the world land mass into regions based on main river basins. Highlighted region in Africa illustrating density of HRUs in the Save Region.

When loaded into the Django visualisation app (Fig. 8), the Web User Interface (UI) showed all gauging stations where the

305 user can pan around and click on any station to see details including performance metrics.



Figure 68: Django Web User Interface for visualising and managing the CoSWAT Global Model (<https://github.com/celray/coswat>)

The web UI also allows users to see which datasets were used, download extract outputs from the model and acts as a

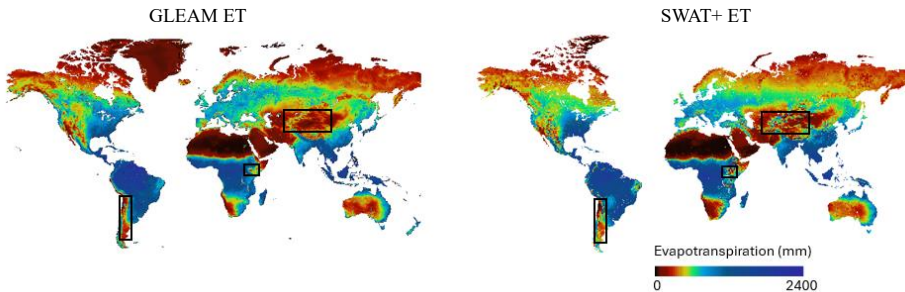
310 calibration portal. Thus, users can extract a region to calibrate and update input files for better model performance.

3.1 Evapotranspiration

A comparison of ET for the effective simulation period (1982 – 1990) shows that the spatial pattern between SWAT+ ET and GLEAM ET is comparable overall (Fig. 9).

315

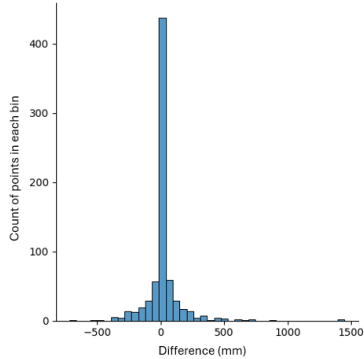
320



325

Figure 79: A comparison of the GLEAM v4 and SWAT+ ET maps. Highlighted regions show artefacts in the SWAT+ Output due to lack of representation of large water bodies and snow issues in high mountains.

However, SWAT+ ET appears to have artefacts on the ET in East Africa (especially in the Ethiopian Highlands) and Central Asia. It also fails to capture the pattern in South America along the Andes mountains. [Figure 8](#)[Figure 10](#) also shows how sampled points compare in differences with 78.54% within the range -100mm to 100mm ET difference.



330

Figure 810: Distribution of differences between GLEAM v4 and SWAT+ simulated mean annual evapotranspiration (ET). The histogram shows the frequency of ET differences, calculated as (GLEAM - SWAT+), at sample points (shown in Figure 6) for the 1982-1990 period.

3.2 River Discharge

335 The model achieved some positive KGE values (23.02%), but a majority of the values were negative as demonstrated by Fig. 11.

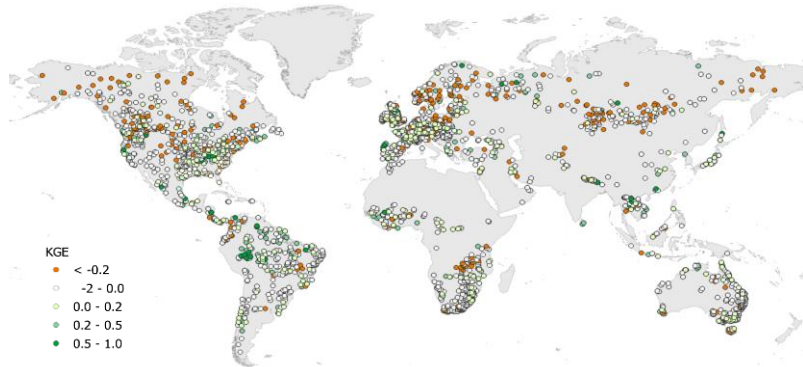


Figure 914: Kling-Gupta Efficiency (KGE) for simulated monthly river discharge (m^3/s) at global gauging stations. The map evaluates the performance of the uncalibrated global SWAT+ model for the 1982-1990 period against GRDC observations.

340 While a small percentage of KGE values were above 0, 85.31% of the stations showed a positive correlation (r) in flow values with variability ratio (α) and mean ratio (β) median values falling close to 1 (Fig. 12).

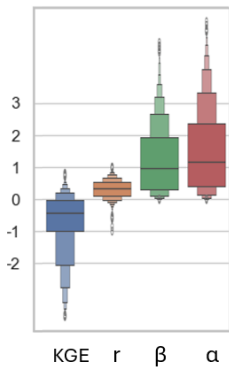


Figure 1042: Distribution of river discharge performance metrics across all evaluated gauging stations. The boxenplots show the statistical distribution of the Kling-Gupta Efficiency (KGE) and its three components: the linear correlation coefficient (r), the variability ratio (α), and the bias ratio (β).

4. Discussion and Future Work

The development of the global SWAT+ model using the CoSWAT framework highlights several significant advancements in large-scale hydrological modelling using SWAT+. The scripted workflow approach offers key advantages. By automating data retrieval, preprocessing, and model configuration within a single framework, the CoSWAT workflow ensures that the

350 model setup can be consistently replicated. This is crucial for verifying results and facilitating collaborative research efforts.

The availability of the workflow as an open-source tool further enhances transparency and community engagement. The CoSWAT framework also efficiently leverages multicore processing capabilities of high-performance computing (HPC) environments which reduces computational time, making it practical to perform high-resolution global simulations that were previously computationally prohibitive (Chawanda et al., 2020b). Users can easily adjust the model setup by modifying the 355 configuration file, allowing for easy updates to input data sources, spatial resolution, or simulation parameters. This flexibility is essential for adapting the model to different research questions or incorporating new datasets as they become available.

With the built in Django App for visualization, the CoSWAT framework plays an important role in visualising results. Users can zoom in to given sections of the model setup to extract and improve model setup separately.

360 The first version of the CoSWAT global model showed promising results despite not being calibrated. The global SWAT+ model demonstrated reasonable performance in simulating ET when compared with the GLEAM v4 dataset. The spatial patterns were generally consistent, with approximately 78.54% of sampled points showing differences within ± 100 mm. However, discrepancies were noted in regions such as East Africa, Central Asia, and along the Andes mountains in South America. A closer look showed excessive snow accumulation in the mountains which can be improved with calibration of 365 SWAT+ snow parameters.

Evaluating differences between modeled and remote-sensing-based ET products involves uncertainties from both sources. Limitations in the resolution or accuracy of input datasets, particularly climate data, can affect ET simulation. Reanalysis datasets may not capture local climate variability effectively, especially in regions with complex topography or sparse

370 observational data (Moalafhi et al., 2017). The absence of lake representation in the SWAT+ Model setup also contributed to some of the discrepancies. For instance, the East African rift valley lake area and big reservoirs in south Africa were all simulated with regular HRUs while implementing lakes and reservoirs would ensure that the land ET and water surface ET are not mixed up to improve spatial Pattern (Fig 9). Concurrently, inherent uncertainties within the GLEAM v4 product itself, potentially related to its algorithms for partitioning ET components such as transpiration vs. soil evaporation, as 375 discussed in studies like Chen et al. (2022), can also influence the comparison results. Thus, there is a need to acknowledge these combined uncertainties when interpreting the evaluation of the ET spatial patterns.

The current effective simulation period (1982 - 1990) was chosen to maximize usable GRDC time series. However, there is very limited eddy covariance (EC) data for further evaluation of model performance in simulating ET. Since calibration and validation were beyond the scope of this study, future studies should make simulations aligned to any available EC data and 380 explore its use for calibration and validation.

The model's performance in simulating river discharge was less satisfactory, with only 23.02% of gauging stations showing positive Kling-Gupta Efficiency (KGE) values for the simulation period (1977 – 1990 with 5 year warm up). Several factors contributed to this outcome. Without calibration, the model relies on default parameters, which may not reflect the 385 hydrological characteristics of diverse global regions. Calibration would help better represent hydrological processes by adjusting model parameters to match observed streamflow and improve performance (Molina-Navarro et al., 2017). However, at such a scale, calibration would not be easily feasible due to computational and data storage requirements. Chawanda et al 2020 detail how Hydrological Mass Balance Calibration (HMBC) applied at large scale improves water balance representation while also improving model performance in several gauging stations in at a feasible computational 390 cost. This is demonstrated by their application of HMBC on the SWAT+ Model for Africa (Chawanda 2024). Global modelling exercises like CoSWAT global model can also incorporate such calibration routines to improve the model performance.

The non-inclusion of reservoirs and water management practices also negatively affected the performance of the model. The 395 model did not implement reservoirs or account for human interventions such as irrigation, which significantly impact river flow regimes. Large-scale hydrological models struggle with representing human activities accurately due to their complexity and data requirements (Wada et al., 2017). Including reservoirs and management practices is an important part for realistic flow simulations, as demonstrated by Chawanda et al. (2020a), who showed that incorporating these elements improves river flow and ET simulations.

400 Poor performance was also noted in higher latitudes which may be attributed to excessive simulation of snow, leading to overestimated flows. This suggests a need to refine the model's snow routines or adjust parameters related to cold climate processes. While snow related performance issues are specific to high latitude areas, the use of reanalysis climate data at a 0.5-degree likely caused reduced model performance throughout the model setup. The 0.5-degree resolution may not capture 405 local-scale climate variations, particularly in regions with significant topographic variability (Kay et al., 2015). Downscaling techniques or higher-resolution datasets could enhance model performance (Wang et al., 2020; Zhu et al., 2023). One major limitation faced during the simulation of the global model, the current SWAT+ climate input system requires individual files for each variable at each weather station, resulting in a massive number of files for global models. In our Model Setup, we required about 230,000 climate files at 0.5 decimal degree resolution. This approach strains computational resources, slows 410 disk access, and increases memory usage, especially for long-term simulations or multiple scenarios and limits applicability

of downscaling efforts. There is a need to modify the input system to handle large datasets more efficiently by adopting and integrating more efficient file formats like NetCDF which would only need one file for all timesteps and climate variables.

Future model versions should include reservoirs, irrigation, and other water management practices to capture both natural and anthropogenic activities. This requires collection of global datasets on water infrastructure and usage, which can be challenging but is essential for better process representation (Nkwasa et al., 2022a). In addition, HMBC should be employed to further improve process representation and hence model performance. Snow process and parameters also need to be revised to prevent snow build up in higher latitudes.

Finally, while placing model performance in the context of established global models like those within the ISIMIP ensemble is valuable, a direct quantitative comparison of river discharge statistics (e.g., KGE) was considered beyond the scope of this initial study and potentially misleading due to fundamental differences in model resolution. Comparing our high-resolution outputs, which capture finer-scale heterogeneity, against typical ISIMIP model outputs (0.5-degree) at specific gauge locations requires careful consideration of scale mismatches. Future work could explore methodologies for robust inter-comparison that account for these scale differences, potentially leveraging the aggregation capabilities of the CoSWAT framework.

5. Conclusions

The development of a high-resolution global SWAT+ model using the CoSWAT framework marks a significant step forward in global hydrological modelling. The framework's reproducibility, scalability, and flexibility address many challenges associated with large-scale simulations. While the model performed well in simulating evapotranspiration, discrepancies in certain regions highlight the need for further refinement of input data and model parameters.

The poor performance in river discharge simulations highlights the importance of model calibration and the inclusion of human activities such as reservoir operations and water management practices. Future work should focus on enhancing the representation of critical hydrological processes, integrating human interventions, and improving input data quality and resolution. Adopting more efficient data handling strategies within the SWAT+ framework will also facilitate larger and more complex simulations. By addressing these challenges, the global SWAT+ model can become a powerful tool for understanding global water resources and easily map hotspots for water scarcity, assessing CC and land use impacts, and supporting sustainable water management practices worldwide.

Code and data availability

Simulations have a large size and cannot easily be hosted online. However, they are available upon request. The tools used in this study are available from github (<https://github.com/celray/CoSWAT-Framework> and <https://github.com/celray/coswat>,

last access: 28 December 2024) and through Zenodo at <https://zenodo.org/doi/10.5281/zenodo.14577842> (Chawanda, 2024).

All input data is from open sources as discussed in the manuscript.

Acknowledgements

The authors thank the Research Foundation – Flanders (FWO) for funding the International Coordination Action (ICA)

445 “Open Water Network: Open Data and Software tools for water resources management” (project code G0E2621N), the Open Water Network: impacts of global change on water quality (project code G0ADS24N), the AXA Research Chair fund on Water Quality and Global change and the King Baudouin Foundation for the Ernest du Bois Prize Fund (agreement No. 2022-F2812650-228938).

450 **Author contributions** CJC conceptualized the study, performed the investigation and analysis. All authors contributed to the result interpretation and review. CJC wrote the first draft of the manuscript, and all authors commented and revised the manuscript. All authors read and approved the final manuscript.

Competing interests

455 The authors declare that they have no conflict of interest.

References

Abbaspour, K. C., Rouholahnejad, E., Vaghefi, S., Srinivasan, R., Yang, H., and Kløve, B.: A continental-scale hydrology and water quality model for Europe: Calibration and uncertainty of a high-resolution large-scale SWAT model, *J. Hydrol.*, 524, 733–752, <https://doi.org/10.1016/j.jhydrol.2015.03.027>, 2015.

460 Alemayehu, T., Van Griensven, A., Woldegiorgis, B. T., and Bauwens, W.: An improved SWAT vegetation growth module and its evaluation for four tropical ecosystems, *Hydrol. Earth Syst. Sci.*, 21, 4449–4467, <https://doi.org/10.5194/hess-21-4449-2017>, 2017.

465 Amjath-Babu, T. S., Sharma, B., Brouwer, R., Rasul, G., Wahid, S. M., Neupane, N., Bhattacharai, U., and Sieber, S.: Integrated modelling of the impacts of hydropower projects on the water-food-energy nexus in a transboundary Himalayan river basin, *Appl. Energy*, 239, 494–503, <https://doi.org/10.1016/j.apenergy.2019.01.147>, 2019.

SWAT Global Data: <https://swat.tamu.edu/data/>, last access: 23 September 2025.

Anon: GRDC, n.d.

Arnold, J., Bieger, K., White, M., Srinivasan, R., Dunbar, J., and Allen, P.: Use of Decision Tables to Simulate Management in SWAT, *Water*, 10, 713, <https://doi.org/10.3390/W10060713>, 2018.

470 Becher, O., Smilovic, M., Verschuur, J., Pant, R., Tramberend, S., and Hall, J.: The challenge of closing the climate adaptation gap for water supply utilities, *Commun. Earth Environ.*, 5, 356, <https://doi.org/10.1038/s43247-024-01272-3>, 2024.

475 Best, M. J., Pryor, M., Clark, D. B., Rooney, G. G., Essery, R. L. H., Ménard, C. B., Edwards, J. M., Hendry, M. A., Porson, A., Gedney, N., Mercado, L. M., Sitch, S., Blyth, E., Boucher, O., Cox, P. M., Grimmond, C. S. B., and Harding, R. J.: The Joint UK Land Environment Simulator (JULES), Model description – Part 1: Energy and water fluxes, <https://doi.org/10.5194/gmdd-4-595-2011>, 24 March 2011.

Bieger, K., Arnold, J. G., Rathjens, H., White, M. J., Bosch, D. D., Allen, P. M., Volk, M., and Srinivasan, R.: Introduction to SWAT+, a completely restructured version of the soil and water assessment tool, *JAWRA J. Am. Water Resour. Assoc.*, 53, 115–130, 2017.

480 Brunner, M. I., Slater, L., Tallaksen, L. M., and Clark, M.: Challenges in modeling and predicting floods and droughts: A review, *WIREs Water*, 8, e1520, <https://doi.org/10.1002/wat2.1520>, 2021.

Burek, P., Satoh, Y., Kahil, T., Tang, T., Greve, P., Smilovic, M., Guillaumot, L., Zhao, F., and Wada, Y.: Development of the Community Water Model (CWatM v1.04) – a high-resolution hydrological model for global and regional assessment of integrated water resources management, *Geosci. Model Dev.*, 13, 3267–3298, <https://doi.org/10.5194/gmd-13-3267-2020>, 485 2020.

Chawanda, C. J.: CoSWAT Framework, <https://doi.org/10.5281/ZENODO.14577842>, 2024.

Chawanda, C. J., Arnold, J., Thiery, W., and Van Griensven, A.: Mass balance calibration and reservoir representations for large-scale hydrological impact studies using SWAT+, *Clim. Change*, 163, 1307–1327, <https://doi.org/10.1007/s10584-020-02924-x>, 2020a.

490 Chawanda, C. J., George, C., Thiery, W., Griensven, A. V., Tech, J., Arnold, J., and Srinivasan, R.: User-friendly workflows for catchment modelling: Towards reproducible SWAT+ model studies, *Environ. Model. Softw.*, 134, 104812, <https://doi.org/10.1016/j.envsoft.2020.104812>, 2020b.

Chawanda, C. J., Nkwasa, A., Thiery, W., and Van Griensven, A.: Combined impacts of climate and land-use change on future water resources in Africa, <https://doi.org/10.5194/hess-2023-93>, 8 January 2024.

495 Chen, H., Zhu, G., Shang, S., Qin, W., Zhang, Y., Su, Y., Zhang, K., Zhu, Y., and Xu, C.: Uncertainties in partitioning evapotranspiration by two remote sensing-based models, *J. Hydrol.*, 604, 127223, <https://doi.org/10.1016/j.jhydrol.2021.127223>, 2022.

Crochemore, L., Isberg, K., Pimentel, R., Pineda, L., Hasan, A., and Arheimer, B.: Lessons learnt from checking the quality of openly accessible river flow data worldwide, *Hydrol. Sci. J.*, 65, 699–711, 500 <https://doi.org/10.1080/02626667.2019.1659509>, 2020.

Defourny, P., Lamarche, C., Bontemps, S., De Maet, T., Van Bogaert, E., Moreau, I., Brockmann, C., Boettcher, M., Kirches, G., Wevers, J., and Santoro, M.: Land Cover CCI: Product User Guide, Version 2.0, European Space Agency (ESA) and UCL-Geomatics, Louvain-la-Neuve, Belgium, 2017.

Döll, P., Douville, H., Güntner, A., Müller Schmied, H., and Wada, Y.: Modelling Freshwater Resources at the Global Scale: 505 Challenges and Prospects, *Surv. Geophys.*, 37, 195–221, <https://doi.org/10.1007/s10712-015-9343-1>, 2016.

Dottori, F., Szewczyk, W., Ciscar, J.-C., Zhao, F., Alfieri, L., Hirabayashi, Y., Bianchi, A., Mongelli, I., Frieler, K., Betts, R. A., and Feyen, L.: Increased human and economic losses from river flooding with anthropogenic warming, *Nat. Clim. Change*, 8, 781–786, <https://doi.org/10.1038/s41558-018-0257-z>, 2018.

510 Fischer, G., Nachtergaele, F., Prieler, S., van Velthuizen, H. T., Verelst, L., and Wiberg, D.: Global Agro-ecological Zones Assessment for Agriculture (GAEZ 2008), IIASA, Laxenburg, Austria and FAO, Rome, Italy, 2008.

Fu, B., Merritt, W. S., Croke, B. F. W., Weber, T. R., and Jakeman, A. J.: A review of catchment-scale water quality and erosion models and a synthesis of future prospects, *Environ. Model. Softw.*, 114, 75–97, <https://doi.org/10.1016/j.envsoft.2018.12.008>, 2019.

515 Gosling, S. N., Schmied, H. M., Betts, R., Chang, J., Chen, H., Ciais, P., Dankers, R., Döll, P., Eisner, S., Flörke, M., Gerten, D., Grillakis, M., Hagemann, S., Hanasaki, N., Huang, M., Huang, Z., Jerez, S., Kim, H., Koutroulis, A., Leng, G., Liu, J., Liu, X., Mao, G., Masaki, Y., Montavez, J. P., Morfopoulos, C., Oki, T., Orth, R., Ostberg, S., Papadimitriou, L., Pokhrel, Y., Portmann, F., Qi, W., Satoh, Y., Seneviratne, S., Sommer, P. S., Stacke, T., Tang, Q., Tsanis, I., Wada, Y., Wang, X., Zhou, T., Büchner, M., Schewe, J., and Zhao, F.: ISIMIP2a Simulation Data from the Global Water Sector (2.0), <https://doi.org/10.48364/ISIMIP.882536>, 2023a.

520 Gosling, S. N., Schmied, H. M., Burek, P., Chang, J., Ciais, P., Döll, P., Eisner, S., Fink, G., Flörke, M., Franssen, W., Grillakis, M., Hagemann, S., Hanasaki, N., Koutroulis, A., Leng, G., Liu, X., Masaki, Y., Mathison, C., Mishra, V., Ostberg, S., Portmann, F., Qi, W., Sahu, R.-K., Satoh, Y., Schewe, J., Seneviratne, S., Shah, H. L., Stacke, T., Tao, F., Telteu, C., Thiery, W., Trautmann, T., Tsanis, I., Wanders, N., Zhai, R., Büchner, M., and Zhao, F.: ISIMIP2b Simulation Data from the Global Water Sector (1.0), <https://doi.org/10.48364/ISIMIP.626689>, 2023b.

525 Gosling, S. N., Müller Schmied, H., Bradley, A., Burek, P., Chang, J., Ciais, P., Grillakis, M., Guillaumot, L., Hanasaki, N., Hartley, A., Huang, H., Kou-Giesbrecht, S., Koutroulis, A., Otta, K., Satoh, Y., Stacke, T., Zhu, Q., and Schewe, J.: ISIMIP3a Simulation Data from the Global Water Sector (1.3), <https://doi.org/10.48364/ISIMIP.398165.3>, 2024a.

530 Gosling, S. N., Müller Schmied, H., Burek, P., Guillaumot, L., Hanasaki, N., Kou-Giesbrecht, S., Otta, K., Sahu, R.-K., Satoh, Y., and Schewe, J.: ISIMIP3b Simulation Data from the Global Water Sector (1.1), <https://doi.org/10.48364/ISIMIP.230418.1>, 2024b.

Gudmundsson, L., Boulange, J., Do, H. X., Gosling, S. N., Grillakis, M. G., Koutroulis, A. G., Leonard, M., Liu, J., Müller Schmied, H., Papadimitriou, L., Pokhrel, Y., Seneviratne, S. I., Satoh, Y., Thiery, W., Westra, S., Zhang, X., and Zhao, F.: Globally observed trends in mean and extreme river flow attributed to climate change, *Science*, 371, 1159–1162, <https://doi.org/10.1126/science.aba3996>, 2021.

535 Guimbertea, M., Ducharne, A., Ciais, P., Boisier, J. P., Peng, S., De Weirdt, M., and Verbeeck, H.: Testing conceptual and physically based soil hydrology schemes against observations for the Amazon Basin, *Geosci. Model Dev.*, 7, 1115–1136, <https://doi.org/10.5194/gmd-7-1115-2014>, 2014.

540 Guimbertea, M., Zhu, D., Maignan, F., Huang, Y., Yue, C., Dantec-Nédélec, S., Ottlé, C., Jornet-Puig, A., Bastos, A., Laurent, P., Goll, D., Bowring, S., Chang, J., Guenet, B., Tifafi, M., Peng, S., Krinner, G., Ducharne, A., Wang, F., Wang, T., Wang, X., Wang, Y., Yin, Z., Lauerwald, R., Joetzjer, E., Qiu, C., Kim, H., and Ciais, P.: ORCHIDEE-MICT (revision 4126), a land surface model for the high-latitudes: model description and validation, <https://doi.org/10.5194/gmd-2017-122>, 16 June 2017.

545 Gupta, H. V., Kling, H., Yilmaz, K. K., and Martinez, G. F.: Decomposition of the mean squared error and NSE performance criteria: Implications for improving hydrological modelling, *J. Hydrol.*, 377, 80–91, <https://doi.org/10.1016/j.jhydrol.2009.08.003>, 2009.

Haddeland, I., Clark, D. B., Franssen, W., Ludwig, F., Voß, F., Arnell, N. W., Bertrand, N., Best, M., Folwell, S., Gerten, D., Gomes, S., Gosling, S. N., Hagemann, S., Hanasaki, N., Harding, R., Heinke, J., Kabat, P., Koitala, S., Oki, T., Polcher, J., Stacke, T., Viterbo, P., Weedon, G. P., and Yeh, P.: Multimodel Estimate of the Global Terrestrial Water Balance: Setup and First Results, *J. Hydrometeorol.*, 12, 869–884, <https://doi.org/10.1175/2011JHM1324.1>, 2011.

550 Hanasaki, N., Yoshikawa, S., Pokhrel, Y., and Kanae, S.: A global hydrological simulation to specify the sources of water used by humans, *Hydrol. Earth Syst. Sci.*, 22, 789–817, <https://doi.org/10.5194/hess-22-789-2018>, 2018a.

Hanasaki, N., Yoshikawa, S., Pokhrel, Y., and Kanae, S.: A Quantitative Investigation of the Thresholds for Two Conventional Water Scarcity Indicators Using a State-of-the-Art Global Hydrological Model With Human Activities, *Water Resour. Res.*, 54, 8279–8294, <https://doi.org/10.1029/2018WR022931>, 2018b.

555 Huang, H., Xue, Y., Li, F., and Liu, Y.: Modeling long-term fire impact on ecosystem characteristics and surface energy using a process-based vegetation–fire model SSiB4/TRIFFID-Fire v1.0, *Geosci. Model Dev.*, 13, 6029–6050, <https://doi.org/10.5194/gmd-13-6029-2020>, 2020.

560 Kay, A. L., Rudd, A. C., Davies, H. N., Kendon, E. J., and Jones, R. G.: Use of very high resolution climate model data for hydrological modelling: baseline performance and future flood changes, *Clim. Change*, 133, 193–208, <https://doi.org/10.1007/s10584-015-1455-6>, 2015.

Kew, S. F., Philip, S. Y., Hauser, M., Hobbins, M., Wanders, N., van Oldenborgh, G. J., van der Wiel, K., Veldkamp, T. I. E., Kimutai, J., Funk, C., and Otto, F. E. L.: Impact of precipitation and increasing temperatures on drought trends in eastern Africa, *Earth Syst. Dyn.*, 12, 17–35, <https://doi.org/10.5194/esd-12-17-2021>, 2021.

565 Knoben, W. J. M., Clark, M. P., Bales, J., Bennett, A., Gharari, S., Marsh, C. B., Nijssen, B., Pietroniro, A., Spiteri, R. J., Tang, G., Tarboton, D. G., and Wood, A. W.: Community Workflows to Advance Reproducibility in Hydrologic Modeling: Separating Model-Agnostic and Model-Specific Configuration Steps in Applications of Large-Domain Hydrologic Models, *Water Resour. Res.*, 58, e2021WR031753, <https://doi.org/10.1029/2021WR031753>, 2022.

Lange, S. and Büchner, M.: ISIMIP2a atmospheric climate input data (1.0), <https://doi.org/10.48364/ISIMIP.886955>, 2020.

570 Lawrence, D. M., Fisher, R. A., Koven, C. D., Oleson, K. W., Swenson, S. C., Bonan, G., Collier, N., Ghimire, B., Van Kampenhout, L., Kennedy, D., Kluzek, E., Lawrence, P. J., Li, F., Li, H., Lombardozzi, D., Riley, W. J., Sacks, W. J., Shi, M., Vertenstein, M., Wieder, W. R., Xu, C., Ali, A. A., Badger, A. M., Bish, G., Van Den Broeke, M., Brunke, M. A., Burns, S. P., Buzan, J., Clark, M., Craig, A., Dahl, K., Drewniak, B., Fisher, J. B., Flanner, M., Fox, A. M., Gent, P., Hoffman, F., Keppel-Aleks, G., Knox, R., Kumar, S., Lenaerts, J., Leung, L. R., Lipscomb, W. H., Lu, Y., Pandey, A., Pelletier, J. D., Perket, J., Randerson, J. T., Ricciuto, D. M., Sanderson, B. M., Slater, A., Subin, Z. M., Tang, J., Thomas, R. Q., Val Martin, M., and Zeng, X.: The Community Land Model Version 5: Description of New Features, Benchmarking, and Impact of Forcing Uncertainty, *J. Adv. Model. Earth Syst.*, 11, 4245–4287, <https://doi.org/10.1029/2018MS001583>, 2019.

Li, M., Fu, Q., Singh, V. P., Liu, D., Li, T., and Zhou, Y.: Managing agricultural water and land resources with tradeoff between economic, environmental, and social considerations: A multi-objective non-linear optimization model under uncertainty, *Agric. Syst.*, 178, 102685, <https://doi.org/10.1016/j.agsy.2019.102685>, 2020.

580 Liang, X., Lettenmaier, D. P., Wood, E. F., and Burges, S. J.: A simple hydrologically based model of land surface water and energy fluxes for general circulation models, *J. Geophys. Res. Atmospheres*, 99, 14415–14428, <https://doi.org/10.1029/94JD00483>, 1994.

585 Liu, Y., Li, S., Wallace, C. W., Chaubey, I., Flanagan, D. C., Theller, L. O., and Engel, B. A.: Comparison of Computer Models for Estimating Hydrology and Water Quality in an Agricultural Watershed, *Water Resour. Manag.*, 31, 3641–3665, <https://doi.org/10.1007/s11269-017-1691-9>, 2017.

Ma, J., Zheng, H., Li, R., Rao, K., Yang, Y., and Li, W.: A Hadoop cloud-based surrogate modelling framework for approximating complex hydrological models, *J. Hydroinformatics*, 25, 511–525, <https://doi.org/10.2166/hydro.2023.184>, 2023.

590 Ma, T., Duan, Z., Li, R., and Song, X.: Enhancing SWAT with remotely sensed LAI for improved modelling of ecohydrological process in subtropics, *J. Hydrol.*, 570, 802–815, <https://doi.org/10.1016/j.jhydrol.2019.01.024>, 2019.

Mao, G. and Liu, J.: WAYS v1: a hydrological model for root zone water storage simulation on a global scale, *Geosci. Model Dev.*, 12, 5267–5289, <https://doi.org/10.5194/gmd-12-5267-2019>, 2019.

595 Melton, J. R., Arora, V. K., Wisernig-Cojoc, E., Seiler, C., Fortier, M., Chan, E., and Teckentrup, L.: CLASSIC v1.0: the open-source community successor to the Canadian Land Surface Scheme (CLASS) and the Canadian Terrestrial Ecosystem Model (CTEM) – Part 1: Model framework and site-level performance, *Geosci. Model Dev.*, 13, 2825–2850, <https://doi.org/10.5194/gmd-13-2825-2020>, 2020.

Miralles, D. G., Bonte, O., Koppa, A., Baez-Villanueva, O. M., Tronquo, E., Zhong, F., Beck, H. E., Hulsman, P., Dorigo, W., Verhoest, N. E. C., and Haghdoost, S.: GLEAM4: global land evaporation and soil moisture dataset at 0.1° resolution from 1980 to near present, *Sci. Data*, 12, 416, <https://doi.org/10.1038/s41597-025-04610-y>, 2025.

600 Moalafhi, D. B., Sharma, A., and Evans, J. P.: Reconstructing hydro-climatological data using dynamical downscaling of reanalysis products in data-sparse regions – Application to the Limpopo catchment in southern Africa, *J. Hydrol. Reg. Stud.*, 12, 378–395, <https://doi.org/10.1016/j.ejrh.2017.07.001>, 2017.

605 Molina-Navarro, E., Andersen, H. E., Nielsen, A., Thodsen, H., and Trolle, D.: The impact of the objective function in multi-site and multi-variable calibration of the SWAT model, *Environ. Model. Softw.*, 93, 255–267, <https://doi.org/10.1016/j.envsoft.2017.03.018>, 2017.

Muheki, D., Dejins, A. A. J., Bevacqua, E., Messori, G., Zscheischler, J., and Thiery, W.: The perfect storm? Co-occurring climate extremes in East Africa, *Earth Syst. Dyn.*, 15, 429–466, <https://doi.org/10.5194/esd-15-429-2024>, 2024.

610 Müller Schmied, H., Cáceres, D., Eisner, S., Flörke, M., Herbert, C., Niemann, C., Peiris, T. A., Popat, E., Portmann, F. T., Reinecke, R., Schumacher, M., Shadkam, S., Telteu, C.-E., Trautmann, T., and Döll, P.: The global water resources and use model WaterGAP v2.2d: model description and evaluation, *Geosci. Model Dev.*, 14, 1037–1079, <https://doi.org/10.5194/gmd-14-1037-2021>, 2021.

Nkwasa, A., Chawanda, C. J., Jägermeyr, J., and Van Griensven, A.: Improved representation of agricultural land use and crop management for large-scale hydrological impact simulation in Africa using SWAT+, *Hydrol. Earth Syst. Sci.*, 26, 71–89, <https://doi.org/10.5194/hess-26-71-2022>, 2022a.

615 Nkwasa, A., Chawanda, C. J., and Van Griensven, A.: Regionalization of the SWAT+ model for projecting climate change impacts on sediment yield: An application in the Nile basin, *J. Hydrol. Reg. Stud.*, 42, 101152, <https://doi.org/10.1016/j.ejrh.2022.101152>, 2022b.

620 Nkwasa, A., James Chawanda, C., Theresa Nakkazi, M., Tang, T., Eisenreich, S. J., Warner, S., and Van Griensven, A.: One third of African rivers fail to meet the 'good ambient water quality' nutrient targets, *Ecol. Indic.*, 166, 112544, <https://doi.org/10.1016/j.ecolind.2024.112544>, 2024.

Oleson, K., Lawrence, D., Bonan, G., Drewniak, B., Huang, M., Koven, C., Levis, S., Li, F., Riley, W., Subin, Z., Swenson, S., Thornton, P., Bozbayik, A., Fisher, R., Heald, C., Kluzek, E., Lamarque, J.-F., Lawrence, P., Leung, L., Lipscomb, W., Muszala, S., Ricciuto, D., Sacks, W., Sun, Y., Tang, J., and Yang, Z.-L.: Technical description of version 4.5 of the Community Land Model (CLM), UCAR/NCAR, <https://doi.org/10.5065/D6RR1W7M>, 2013.

625 Palazzo, A., Kahil, T., Willaarts, B. A., Burek, P., Van Dijk, M., Tang, T., Magnuszewski, P., Havlik, P., Langan, S., and Wada, Y.: Assessing sustainable development pathways for water, food, and energy security in a transboundary river basin, Environ. Dev., 51, 101030, <https://doi.org/10.1016/j.envdev.2024.101030>, 2024.

Pandi, D., Kothandaraman, S., and Kuppusamy, M.: Simulation of Water Balance Components Using SWAT Model at Sub Catchment Level, Sustainability, 15, 1438, <https://doi.org/10.3390/su15021438>, 2023.

630 Peker, I. and Sorman, A.: Application of SWAT Using Snow Data and Detecting Climate Change Impacts in the Mountainous Eastern Regions of Turkey, Water, 13, 1982, <https://doi.org/10.3390/w13141982>, 2021.

Pokhrel, Y., Felfelani, F., Satoh, Y., Boulange, J., Burek, P., Gädeke, A., Gerten, D., Gosling, S. N., Grillakis, M., Gudmundsson, L., Hanasaki, N., Kim, H., Koutoulis, A., Liu, J., Papadimitriou, L., Schewe, J., Müller Schmied, H., Stacke, T., Telteu, C.-E., Thiery, W., Veldkamp, T., Zhao, F., and Wada, Y.: Global terrestrial water storage and drought severity under climate change, Nat. Clim. Change, 11, 226–233, <https://doi.org/10.1038/s41558-020-00972-w>, 2021.

635 Porkka, M., Virkki, V., Wang-Erlandsson, L., Gerten, D., Gleeson, T., Mohan, C., Fetzer, I., Jaramillo, F., Staal, A., te Wierik, S., Tobian, A., van der Ent, R., Doll, P., Flörke, M., Gosling, S. N., Hanasaki, N., Satoh, Y., Müller Schmied, H., Wanders, N., Famiglietti, J. S., Rockström, J., and Kummu, M.: Notable shifts beyond pre-industrial streamflow and soil moisture conditions transgress the planetary boundary for freshwater change, Nat. Water, 2, 262–273, <https://doi.org/10.1038/s44221-024-00208-7>, 2024.

Pulighe, G., Lupia, F., Chen, H., and Yin, H.: Modeling Climate Change Impacts on Water Balance of a Mediterranean Watershed Using SWAT+, Hydrology, 8, 157, <https://doi.org/10.3390/hydrology8040157>, 2021.

Qi, J., Zhang, X., and Cosh, M. H.: Modeling soil temperature in a temperate region: A comparison between empirical and physically based methods in SWAT, Ecol. Eng., 129, 134–143, <https://doi.org/10.1016/j.ecoleng.2019.01.017>, 2019.

645 Qi, J., Kang, X., Li, S., and Meng, F.: Evaluating Impacts of Detailed Land Use and Management Inputs on the Accuracy and Resolution of SWAT Predictions in an Experimental Watershed, Water, 14, 2352, <https://doi.org/10.3390/w14152352>, 2022a.

650 Qi, W., Feng, L., Yang, H., Liu, J., Zheng, Y., Shi, H., Wang, L., and Chen, D.: Economic growth dominates rising potential flood risk in the Yangtze River and benefits of raising dikes from 1991 to 2015, Environ. Res. Lett., 17, 034046, <https://doi.org/10.1088/1748-9326/ac5561>, 2022b.

Ramteke, G., Singh, R., and Chatterjee, C.: Assessing Impacts of Conservation Measures on Watershed Hydrology Using MIKE SHE Model in the Face of Climate Change, Water Resour. Manag., 34, 4233–4252, <https://doi.org/10.1007/s11269-020-02669-3>, 2020.

655 Reinecke, R., Müller Schmied, H., Trautmann, T., Andersen, L. S., Burek, P., Flörke, M., Gosling, S. N., Grillakis, M., Hanasaki, N., Koutoulis, A., Pokhrel, Y., Thiery, W., Wada, Y., Yusuke, S., and Döll, P.: Uncertainty of simulated groundwater recharge at different global warming levels: a global-scale multi-model ensemble study, Hydrol. Earth Syst. Sci., 25, 787–810, <https://doi.org/10.5194/hess-25-787-2021>, 2021.

Rene Orth and Seneviratne, S. I.: Introduction of a simple-model-based land surface dataset for Europe, *Environ. Res. Lett.*, 10, 044012, <https://doi.org/10.1088/1748-9326/10/4/044012>, 2015.

660 Samimi, M., Mirchi, A., Moriasi, D., Ahn, S., Alian, S., Taghvaeian, S., and Sheng, Z.: Modeling arid/semi-arid irrigated agricultural watersheds with SWAT: Applications, challenges, and solution strategies, *J. Hydrol.*, 590, 125418, <https://doi.org/10.1016/j.jhydrol.2020.125418>, 2020.

665 Sitch, S., Smith, B., Prentice, I. C., Arneth, A., Bondeau, A., Cramer, W., Kaplan, J. O., Levis, S., Lucht, W., Sykes, M. T., Thonnicke, K., and Venevsky, S.: Evaluation of ecosystem dynamics, plant geography and terrestrial carbon cycling in the LPJ dynamic global vegetation model, *Glob. Change Biol.*, 9, 161–185, <https://doi.org/10.1046/j.1365-2486.2003.00569.x>, 2003.

Smith, P., Beven, K., Kretzschmar, A., and Chappell, N.: Developing and documenting a Hydrological Model for reproducible research: A new version of Dynamic TOPMODEL, , <https://doi.org/10.5194/egusphere-egu2020-20790>, 2020.

670 Soltani, F., Javadi, S., Roozbahani, A., Massah Bavani, A. R., Golmohammadi, G., Berndtsson, R., Ghordoyee Milan, S., and Maghsoudi, R.: Assessing Climate Change Impact on Water Balance Components Using Integrated Groundwater–Surface Water Models (Case Study: Shazand Plain, Iran), *Water*, 15, 813, <https://doi.org/10.3390/w15040813>, 2023.

Srivastava, A., Kumari, N., and Maza, M.: Hydrological Response to Agricultural Land Use Heterogeneity Using Variable Infiltration Capacity Model, *Water Resour. Manag.*, 34, 3779–3794, <https://doi.org/10.1007/s11269-020-02630-4>, 2020.

675 Stacke, T. and Hagemann, S.: Development and evaluation of a global dynamical wetlands extent scheme, *Hydrol. Earth Syst. Sci.*, 16, 2915–2933, <https://doi.org/10.5194/hess-16-2915-2012>, 2012.

Stacke, T. and Hagemann, S.: HydroPy (v1.0): a new global hydrology model written in Python, *Geosci. Model Dev.*, 14, 7795–7816, <https://doi.org/10.5194/gmd-14-7795-2021>, 2021.

680 Sutanudjaja, E. H., van Beek, R., Wanders, N., Wada, Y., Bosmans, J. H. C., Drost, N., van der Ent, R. J., de Graaf, I. E. M., Hoch, J. M., de Jong, K., Karsenberg, D., López López, P., Peßenteiner, S., Schmitz, O., Straatsma, M. W., Vannametee, E., Wisser, D., and Bierkens, M. F. P.: PCR-GLOBWB 2: a  arcmin global hydrological and water resources model, *Geosci. Model Dev.*, 11, 2429–2453, <https://doi.org/10.5194/gmd-11-2429-2018>, 2018.

Tabari, H., Hosseinzadehtalaei, P., Thiery, W., and Willems, P.: Amplified Drought and Flood Risk Under Future Socioeconomic and Climatic Change, *Earths Future*, 9, e2021EF002295, <https://doi.org/10.1029/2021EF002295>, 2021.

685 Takata, K., Emori, S., and Watanabe, T.: Development of the minimal advanced treatments of surface interaction and runoff, *Glob. Planet. Change*, 38, 209–222, [https://doi.org/10.1016/S0921-8181\(03\)00030-4](https://doi.org/10.1016/S0921-8181(03)00030-4), 2003.

Tang, Q., Oki, T., Kanae, S., and Hu, H.: The Influence of Precipitation Variability and Partial Irrigation within Grid Cells on a Hydrological Simulation, *J. Hydrometeorol.*, 8, 499–512, <https://doi.org/10.1175/JHM589.1>, 2007.

690 Telteu, C.-E., Müller Schmied, H., Thiery, W., Leng, G., Burek, P., Liu, X., Boulange, J. E. S., Andersen, L. S., Grillakis, M., Gosling, S. N., Satoh, Y., Rakovec, O., Stacke, T., Chang, J., Wanders, N., Shah, H. L., Trautmann, T., Mao, G., Hanasaki, N., Koutoulis, A., Pokhrel, Y., Samaniego, L., Wada, Y., Mishra, V., Liu, J., Döll, P., Zhao, F., Gädeke, A., Rabin, S. S., and Herz, F.: Understanding each other's models: an introduction and a standard representation of 16 global water models to support intercomparison, improvement, and communication, *Geosci. Model Dev.*, 14, 3843–3878, <https://doi.org/10.5194/gmd-14-3843-2021>, 2021.

Thompson, J. R., Gosling, S. N., Zaherpour, J., and Laizé, C. L. R.: Increasing Risk of Ecological Change to Major Rivers of the World With Global Warming, *Earths Future*, 9, e2021EF002048, <https://doi.org/10.1029/2021EF002048>, 2021.

Upadhyay, P., Linhoss, A., Kelble, C., Ashby, S., Murphy, N., and Parajuli, P. B.: Applications of the SWAT Model for Coastal Watersheds: Review and Recommendations, *J. ASABE*, 65, 453–469, <https://doi.org/10.13031/ja.14848>, 2022.

Wada, Y., Bierkens, M. F. P., De Roo, A., Dirmeyer, P. A., Famiglietti, J. S., Hanasaki, N., Konar, M., Liu, J., Müller Schmied, H., Oki, T., Pokhrel, Y., Sivapalan, M., Troy, T. J., Van Dijk, A. I. J. M., Van Emmerik, T., Van Huijgevoort, M. H. J., Van Lanen, H. A. J., Vörösmarty, C. J., Wanders, N., and Wheater, H.: Human–water interface in hydrological modelling: current status and future directions, *Hydrol. Earth Syst. Sci.*, 21, 4169–4193, <https://doi.org/10.5194/hess-21-4169-2017>, 2017.

Wang, Q., Huang, J., Liu, R., Men, C., Guo, L., Miao, Y., Jiao, L., Wang, Y., Shoaib, M., and Xia, X.: Sequence-based statistical downscaling and its application to hydrologic simulations based on machine learning and big data, *J. Hydrol.*, 586, 124875, <https://doi.org/10.1016/j.jhydrol.2020.124875>, 2020.

Yin, Y., Wang, L., Wang, Z., Tang, Q., Piao, S., Chen, D., Xia, J., Conradt, T., Liu, J., Wada, Y., Cai, X., Xie, Z., Duan, Q., Li, X., Zhou, J., and Zhang, J.: Quantifying Water Scarcity in Northern China Within the Context of Climatic and Societal Changes and South-to-North Water Diversion, *Earths Future*, 8, e2020EF001492, <https://doi.org/10.1029/2020EF001492>, 2020.

Yue, L., Shen, H., Zhang, L., Zheng, X., Zhang, F., and Yuan, Q.: High-quality seamless DEM generation blending SRTM-1, ASTER GDEM v2 and ICESat/GLAS observations, *ISPRS J. Photogramm. Remote Sens.*, 123, 20–34, <https://doi.org/10.1016/j.isprsjprs.2016.11.002>, 2017.

Zhang, A., Li, T., Si, Y., Liu, R., Shi, H., Li, X., Li, J., and Wu, X.: Double-layer parallelization for hydrological model calibration on HPC systems, *J. Hydrol.*, 535, 737–747, <https://doi.org/10.1016/j.jhydrol.2016.01.024>, 2016.

Zhou, J., Wu, C., Yeh, P. J.-F., Ju, J., Zhong, L., Wang, S., and Zhang, J.: Anthropogenic climate change exacerbates the risk of successive flood-heat extremes: Multi-model global projections based on the Inter-Sectoral Impact Model Intercomparison Project, *Sci. Total Environ.*, 889, 164274, <https://doi.org/10.1016/j.scitotenv.2023.164274>, 2023.

Zhu, H., Liu, H., Zhou, Q., and Cui, A.: Towards an Accurate and Reliable Downscaling Scheme for High-Spatial-Resolution Precipitation Data, *Remote Sens.*, 15, 2640, <https://doi.org/10.3390/rs15102640>, 2023.

Zhu, Q., Riley, W. J., Tang, J., Collier, N., Hoffman, F. M., Yang, X., and Bisht, G.: Representing Nitrogen, Phosphorus, and Carbon Interactions in the E3SM Land Model: Development and Global Benchmarking, *J. Adv. Model. Earth Syst.*, 11, 2238–2258, <https://doi.org/10.1029/2018MS001571>, 2019.

Zhuang, X. W., Li, Y. P., Nie, S., Fan, Y. R., and Huang, G. H.: Analyzing climate change impacts on water resources under uncertainty using an integrated simulation-optimization approach, *J. Hydrol.*, 556, 523–538, <https://doi.org/10.1016/j.jhydrol.2017.11.016>, 2018.